CDKZM

CRNOGORSKO DRUŠTVO ZA KOROZIJU, ZAŠTITU MATERIJALA I ZAŠTITU ŽIVOTNE SREDINE

PETI MEĐUNARODNI SIMPOZIJUM O KOROZIJI I ZAŠTITI MATERIJALA, ŽIVOTNOJ SREDINI I ZAŠTITI OD POŽARA

KNJIGA RADOVA

FIFTH INTERNATIONAL SYMPOSIUM ON CORROSION AND MATERIALS PROTECTION, ENVIRONMENTAL PROTECTION AND PROTECTION AGAINST FIRE

PROCEEDINGS

Bar, 26-29. septembar 2023. godine

Izdavač
CRNOGORSKO DRUŠTVO ZA KOROZIJU,
ZAŠTITU MATERIJALA I ZAŠTITU ŽIVOTNE SREDINE

Urednik
Prof. dr Darko Vuksanović

CIP - Каталогизација у публикацији
Национална библиотека Црне Горе, Цетиње

ISBN 978-9940-9334-4-9
COBISS.CG-ID 27476484

S A D R Ž A J
C O N T E N T

Nukleacija i rast dendrita kalaja iz alkalnog elektrolita

Nucleation and growth of tin dendrites from alkaline electrolyte

Nebojša D. Nikolić, Jelena D. Lović, Dragana Milošević, Sanja I. Stevanović
Institute of Chemistry, Technology and Metallurgy,
University of Belgrade, Njegoševa 12, 11000 Belgrade, Serbia
Correspondence: nnikolic@ihtm.bg.ac.rs

Izvod

Procesi nukleacije i rasta dendrita kalaja iz alkalnog hidroksidnog elektrolita su istraženi hronoamperometrijom i skenirajućom elektronskom mikroskopskom (SEM) analizom taloga potenciostatski elektrohemijski istaloženih na selektivnim katodnim potencijalima. Za određivanje tipa nukleacije korišćen je model Šarifkera i Hilsa (SH) zasnovan na trodimenzionalnoj nukleaciji sa difuziono kontrolisanim rastom. Bez obzira na primenjeni katodni potencijal, dobijene bezdimenzionalne zavisnosti su bile niže od teorijskih predviđanja za progresivni tip nukleacije. Sa druge strane, morfologija dendrita kalaja je snažno zavisila od primenjenog katodnog potencijala, te igličasti ili dendriti nalik paprati su bili formirani potenciostatskim režimom elektrohemijskog taloženja. Na osnovu morfološke analize Sn dendrita elektrohemijski istaloženih različitim količinama elektriciteta, zaključeno je da nukleacija Sn iz ispitivanog elektrolita ipak sledi progresivni tip, i da se odstupanje od teorijskih predviđanja za ovaj tip može pripisati upotrebi kompleksnog elektrolita za elektrohemijsko taloženje kalaja.

Abstract

The processes of nucleation and growth of tin dendrites from alkaline hydroxide electrolyte have been investigated by chronoamperometry and by the scanning electron microscopic (SEM) analysis of the deposits potentiostatically electrodeposited at the selected cathodic potentials. The Scharifker and Hills (SH) model based on three dimensional nucleation with diffusion controlled growth was used for a determination of a nucleation type. Irrespective of the applied cathodic potential, the obtained dimensionless dependencies were lower than the theoretical predictions for the progressive type of nucleation. On the other hand, morphology of Sn dendrites strongly depended on the applied cathodic potential, and either the needle-like or the fern-like dendrites were formed by the potentiostatic regime of electrodeposition. On the basis of the morphological analysis of Sn dendrites electrodeposited with various amounts of the electricity, it is concluded that nucleation of Sn from the examined electrolyte still follows the progressive type, and that the deviation of the

theoretical predictions for this type can be attributed to use of complex electrolyte for Sn electrodeposition.

Introduction

The dendrites are the most often particle shape of metal powders [1]. For a production of Sn in the form of dendrites, the processes of electrolysis [2–8] and galvanic replacement process [9] are widely used. Electrolysis processes have certain conveniences over all other methods of dendrite production, because shape and size of dendritic particles can be easily controlled by a proper selection of parameters and regimes of the electrodeposition. Simultaneously, electrolysis belongs to environmentally friendly, low cost and time saving method for a metal production [10]. Sn dendrites can be obtained by electrodeposition from both acid [2–4] and alkaline [5–8] electrolytes. The dendrite shape and degree of ramification also depends on the applied regime of electrolysis and the electrolysis time [5,6,8].
Generally, the electrodeposition encompasses the processes of nucleation and growth. Although morphology of Sn dendrites obtained by electrodeposition from alkaline hydroxide electrolyte is relatively well examined [5–8], the best to our knowledge, there is no data about Sn nucleation from this electrolyte. For that reason, the main aim of this study is to examine it and correlate with morphology of Sn dendrites.

Experimental

Tin was electrodeposited from 20 g/L $SnCl_2 \times 2H_2O$ in 250 g/L NaOH at cathodic potentials of –1185, –1200, –1270, –1400, –1600, and –1800 mV vs. Ag/AgCl, and at the room temperature. The time of electrodeposition was 5 s. Electrodeposition of Sn was performed on cylindrical copper electrodes the overall surface area of 0.25 cm^2. The counter electrode was Pt wire, while the reference electrode was Ag/AgCl/3.5 M KCl (in this study, this electrode is denoted as Ag/AgCl). All electrodepositions were performed in a standard three-electrode cell using AUTOLAB potentiostat/galvanostat PGStat 128N (ECO Chemie, The Netherlands). Doubly distilled water and analytical grade chemicals were used for a preparation of solution for Sn electrodeposition. Before the electrodeposition process, the cylindrical Cu electrodes were firstly degreased at a temperature of 70 °C in alkaline detergent, and then etched in 20% H_2SO_4 at 50 °C. After each phase, the Cu electrodes were rinsed with distilled water.
For morphological analysis, Sn was electrodeposited from the same electrolyte at cathodic potentials of –1200 and –1800 mV vs. Ag/AgCl with amounts of the electricity of 200 and 400 mC, and under the same all other electrodeposition

conditions. The produced Sn deposits were characterized by scanning electron microscopy (SEM) technique, using model JEOL JSM-6610LV.

Results and discussion

Figure 1 shows the potentiostatic current transients obtained from 20 g/L $SnCl_2 \times 2H_2O$ in 250 g/L NaOH at cathodic potentials of –1185, –1200, and –1270 mV vs. Ag/AgCl (Fig. 1a), and at –1400, –1600, and –1800 mV vs. Ag/AgCl (Fig. 1b). All the shown $j - t$ dependencies are characterized by the fast increase in the current density, and then by the sharp decrease after reached maximum, and they represent the typical diffusion-limited current transients. The increase in the current density corresponds to the nucleation process and to the growth of already formed nuclei, while the descending part in the current transients until the limiting diffusion current density was reached corresponds to the diffusion controlled growth.

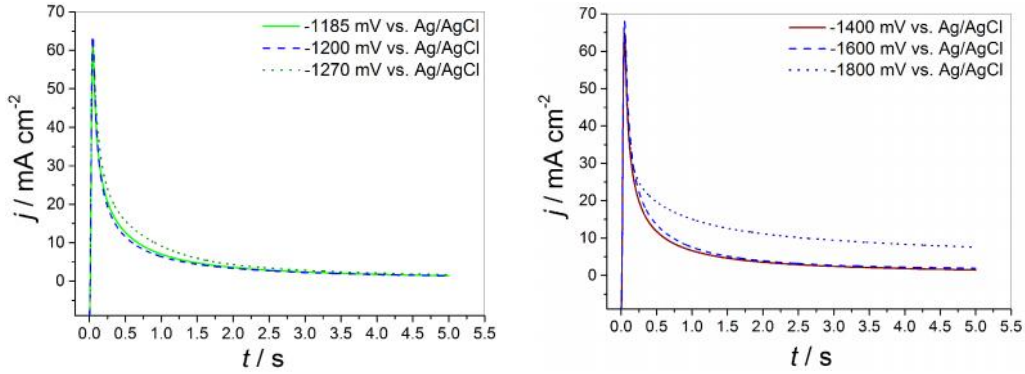

a) *b)*

Figure 1. The potentiostatic current transients recorded at cathodic potentials of: a) –1185, –1200, and –1270 mV vs. Ag/AgCl, and b) –1400, –1600, and –1800 mV vs. Ag/AgCl.

The shape of the potentiostatic current transients, as well as a fact that Sn, together with Pb, Ag, Cd and Zn belongs to the group of so-called the normal metals characterized by the high exchange current density and overpotential for hydrogen discharge values, and the low melting point [11], indicate the possibility of application of the Scharifker and Hills (SH) model [12–15] for a determination of nucleation type. This model, based on the three-dimensional (3D) nucleation and the diffusion-controlled growth, predicts the two limiting types of nucleation: instantaneous and progressive. In the instantaneous type, all nuclei are formed instantaneously, while in the progressive type the number of nuclei is time-dependent and increases with the time.

According to the SH model, the instantaneous and the progressive types of nucleation are described by Equations 1 (instantaneous) and 2 (progressive).

$$\left(\frac{j}{j_m}\right)^2 = \frac{1.9542}{(t/t_m)}\left\{1-\exp\left[-1.2564\left(\frac{t}{t_m}\right)\right]\right\}^2 \quad (1)$$

and

$$\left(\frac{j}{j_m}\right)^2 = \frac{1.2254}{(t/t_m)}\left\{1-\exp\left[-2.3367\left(\frac{t}{t_m}\right)^2\right]\right\}^2 \quad (2)$$

In these Eqs., t_m is a time corresponding to maximal value of the current density, j_m in the potentiostatic current transients. The type of nucleation determines by a comparison of $(j/j_m)^2 - t/t_m$ dependencies derived from the potentiostatic current transients with the theoretical predictions for the SH model.

Figure 2 shows the dimensionless dependencies $(j/j_m)^2 - t/t_m$ derived from the $j - t$ dependencies obtained at various cathodic potentials (Figure 1) and the theoretical predictions for instantaneous and progressive types of nucleation. The obtained dependencies were very similar to each other and lower than the values predicting the progressive type of nucleation.

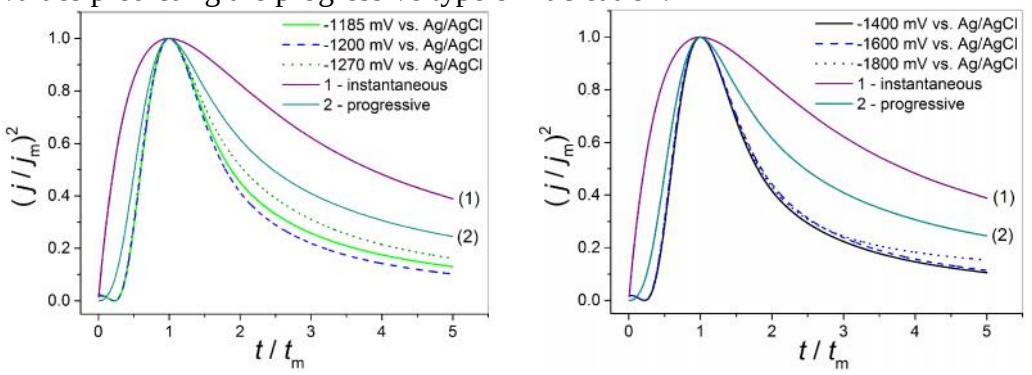

a) *b)*

Figure 2. The dimensionless dependencies $(j/j_m)^2$ J t/t_m obtained by application of SH model for cathodic potentials of: a) –1185, –1200, and –1270 mV vs. Ag/AgCl, and b) –1400, –1600, and –1800 mV vs. Ag/AgCl.

Anyway, the additional analysis was necessary to establish more precisely the nucleation type. The best way to do it is morphological analysis of the deposits obtained by electrodeposition at various cathodic potentials. Figure 3 shows Sn deposits electrodeposited at cathodic potentials of –1200 (Fig. 3a and 3b) and –1800 mV vs. Ag/AgCl (Fig. 3c and 3d) with an amount of the electricity of 200 mC. These cathodic potentials belonged to significantly different positions at the polarization curve for this Sn electrodeposition system [5]. The needle-like dendrites were formed at –1200 mV vs. Ag/AgCl. The two-dimensional (2D) fern-like dendrites growing from one nucleation centre in more directions were

predominately formed at –1800 mV vs. Ag/AgCl. The various sizes of the needle-like dendrites (Fig. 3a and 3b) and the dendrites formed at –1800 mV vs. Ag/AgCl clearly indicate that they are not formed instantaneously and that progressive type of nucleation can be attributed to this Sn electrodeposition system.

The deviations of experimental data from the theoretical prediction for this nucleation type are probably a result of the presence of various complex forms of tin in the alkaline electrolyte [16] and occurring of the additional step in the electrochemical reaction (cation release from the complex at longer deposition times) [3]. The kind of electrolytes also plays a strong role on a nucleation type. For example, a progressive nucleation type occurs from an acid electrolyte with chloride ions, while in the sulfate electrolyte instantaneous type of nucleation can be observed [3].

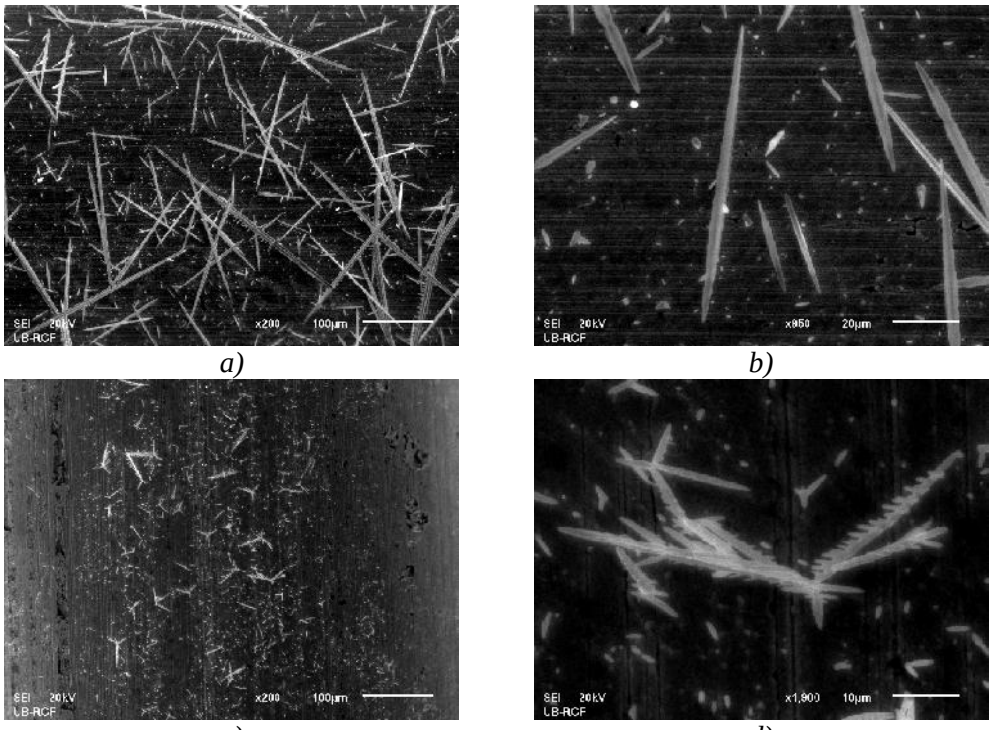

a) *b)*

c) *d)*

Figure 3. Morphology of Sn dendrites electrodeposited from the alkaline hydrohide electrolyte at cathodic potentials of: a) and b) –1200 mV vs. Ag/AgCl, and c) and d) –1800 mV vs. Ag/AgCl. The amount of the electricity: 200 mC.

In the growth process, the current density distribution effect becomes dominant determining the final morphology of electrodeposited metal [1]. Regarding this effect, current lines are primarily concentrated at the higher parts of the electrode surface area, causing the predominant growth on them. In our case, it means that electrodeposition process primarily occurs on initially formed nuclei

and later formed dendrites than at a rest of the electrode surface area. As a result of this effect, in the growth process, the needle-like dendrites of significantly different sizes and the intertwined network of the fern-like dendrites were formed at cathodic potentials of –1200 (Fig. 4a) and –1800 mV vs. Ag/AgCl (Fig. 4b) with twice larger amount of the electricity (i.e. with 400 mC).

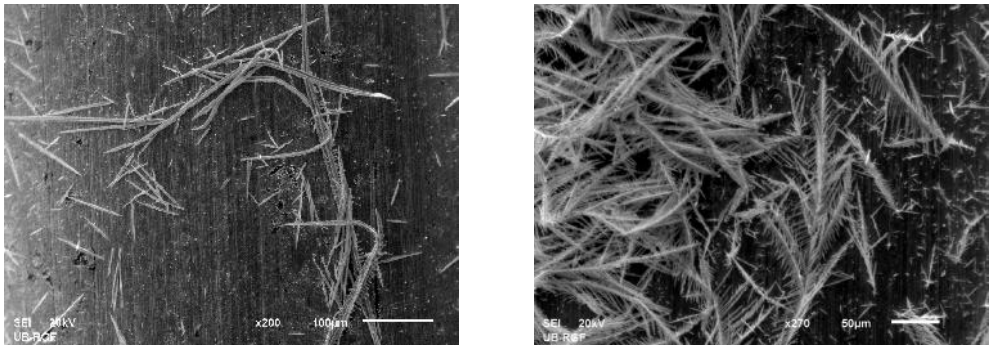

a) *b)*

Figure 4. Morphology of Sn dendrites electrodeposited from the alkaline hydrohide electrolyte at cathodic potentials of: a) –1200 mV vs. Ag/AgCl, and b) –1800 mV vs. Ag/AgCl. The amount of the electricity: 400 mC.

Conclusions

Nucleation and growth of Sn dendrites from the alkaline hydroxide electrolyte has been analysed. Nucleation processes were analysed applying Scharifker and Hills (SH) model based on the three-dimensional (3D) nucleation and the diffusion-controlled growth. The growth process was examined by morphological analysis of Sn dendrites potentiostatically electrodeposited at the various cathodic potentials. In this study, it is shown:

- Irrespective of the applied cathodic potentials, the dimensionless dependencies calculated according to SH model were smaller than those predicting the progressive type of nucleation.
- Morphology of Sn dendrites strongly depended on the applied cathodic potential: the needle-like dendrites of various sizes were formed at lower (–1200 mV vs. Ag/AgCl) and intertwined network of the fern-like dendrites at higher (–1800 mV vs. Ag/AgCl) cathodic potentials.
- The deviations from the theoretical predictions for the progressive type of nucleation are ascribed to use of the complex electrolyte for Sn electrodeposition and consequently, to additional steps in the electrochemical reaction.

Acknowledgement: This research was funded by the Ministry of Science, Technological Development and Innovation of the Republic of Serbia (contract

No. 451-03-47/2023-01/200026) and by the Science Fund of the Republic of Serbia under grant No. 7739802.

References:

[1]. K.I. Popov, S.S. Djokić, N.D. Nikolić, V.D. Jović, *Morphology of Electrochemically and Chemically Deposited Metals*; Springer: New York, NY, USA, 2016; pp. 1–368.
[2]. T.H. Kim, K.S. Hong, D.R. Sohn, M.J. Kim, D.H. Nam, E.A. Cho, H.S. Kwon**,** J. Mater. Chem. A **5** (2017) 20304–20315.
[3]. E. Rudnik, G. Włoch, App. Surf. Sci. **265** (2013) 839–849.
[4]. H.C. Shin, J. Dong, M. Liu, Adv. Mater. **15** (2003) 1610–1614.
[5]. N.D. Nikolić, J.D. Lović, V.M. Maksimović, P.M. Živković, Metals **12** (2022) 1201.
[6]. N.D. Nikolić, J.D. Lović, V.M. Maksimović, J. Solid State Electrochem. **27** (2023) 1889–1900.
[7]. J.D. Lović, S. Eraković Pantović, L.Z. Rakočević, N.L. Ignjatović, S.B. Dimitrijević, N.D. Nikolić, Processes **11** (2023) 120.
[8]. J.D. Lović, N.D. Nikolić, P.M. Živković, S.B. Dimitrijević, M. Stevanović, Maced. J. Chem. Chem. Eng. **42** (2023) 93–102.
[9]. J. Dong, F. Wu, Q. Han, J. Qi, W. Gao, Y. Wang, Tuo. Li, Y. Yang, M. Sun, RSC Adv. **10** (2020) 36042–36050.
[10]. M. Amiri, S. Nouhi, Y. Azizian-Kalandaragh, Mater. Chem. Phys. **155** (2015) 129–135.
[11]. R. Winand, Electrochim. Acta **39** (1994) 1091–1105.
[12]. B. Scharifker, G. Hills, Electrochim. Acta **28** (1983) 879–889.
[13]. B. Scharifker, J. Mostany, J. Electroanal. Chem. **177** (1984) 13–23.
[14]. J. Mostany, J. Mozota, B. Scharifker, **177** (1984) 25–37.
[15]. N.D. Nikolić, S.I. Stevanović, G. Branković, Trans. Nonferrous Met. Soc. China **26** (2016) 3274–3282.
[16]. X. Zhong, L. Chen, B. Medgyes, Z. Zhang, S. Gao, L. Jakab, RSC Adv. **7** (2017) 28186–28206.